

Vortex profiles and vortex interactions at the electroweak crossover*

M.N. Chernodub^a, E.-M. Ilgenfritz^b and A. Schiller^c

^a Institute of Theoretical and Experimental Physics, B. Chermushkinskaya 25, Moscow, 117259, Russia

^b Institute for Theoretical Physics, Kanazawa University, Kanazawa 920-1192, Japan

^c Institut für Theoretische Physik and NTZ, Universität Leipzig, D-04109 Leipzig, Germany

Local correlations of Z -vortex operators with gauge and Higgs fields (lattice quantum vortex profiles) as well as vortex two-point functions are studied in the crossover region near a Higgs mass of 100 GeV within the $3D$ $SU(2)$ Higgs model. The vortex profiles resemble certain features of the classical vortex solutions in the continuum. The vortex-vortex interactions are analogous to the interactions of Abrikosov vortices in a type-I superconductor.

1. Introduction

Although the standard model does not possess *topologically stable* monopole- and vortex-like defects, one can define so-called *embedded* topological defects [1,2]: Nambu monopoles [3] and Z -vortex strings [3,4]. Last year, we have started [5,6] to investigate how the electroweak transition and the continuous crossover can be understood in terms of the behavior of these excitations. This has been done in the framework of dimensional reduction which is reliable for Higgs boson masses between 30 and 240 GeV [7]. Due to the similarity of the phase transitions in the $SU(2)$ Higgs model and in the $SU(2) \times U(1)$ electroweak theory [8], we restricted ourselves to the $3D$ $SU(2)$ Higgs model.

In our lattice studies [5] we observed the vortices to undergo a so-called percolation transition which coincides with the first order phase transition at small Higgs masses. The percolation transition continues to exist at realistic (large) Higgs mass [6] when the electroweak theory has a smooth crossover rather than a true thermal phase transition [9]. In our present study we have a closer look at the vortex properties within the electroweak crossover regime [for a Higgs boson mass ≈ 103 GeV (94 GeV) in a $4D$ $SU(2)$ Higgs model with (without) top quark].

2. Lattice model and defect operators

To construct the vortices on the lattice we use their correspondence to the Abrikosov-Nielsen-Olesen (ANO) strings [10] embedded into an Abelian subgroup of the $SU(2)$ gauge group. We define a composite adjoint unit vector field $n_x = n_x^a \sigma^a$, $n_x^a = -(\phi_x^+ \sigma^a \phi_x) / (\phi_x^+ \phi_x)$, where the 2-component complex isospinor ϕ_x is the Higgs field. The field n allows to define the gauge invariant flux $\bar{\theta}_p$ through the plaquette $p = \{x, \mu\nu\}$ as $\bar{\theta}_p = \arg(\text{Tr}[(\mathbb{1} + n_x) V_{x,\mu} V_{x+\hat{\mu},\nu} V_{x+\hat{\nu},\mu}^+ V_{x,\nu}^+])$ where $V_{x,\mu}(U, n) = U_{x,\mu} + n_x U_{x,\mu} n_{x+\hat{\mu}}$ is the projection of a link. Abelian link angles $\chi_{x,\mu} = \arg(\phi_x^+ V_{x,\mu} \phi_{x+\hat{\mu}})$ are used to construct a plaquette angle $\chi_p = \chi_{x,\mu} + \chi_{x+\hat{\mu},\nu} - \chi_{x+\hat{\nu},\mu} - \chi_{x,\nu}$. The vorticity σ_p on the plaquette p is [11]:

$$\sigma_p = (\chi_p - \bar{\theta}_p) / (2\pi). \quad (1)$$

The vortex trajectories are formed by links $^*l = \{x, \rho\}$ of the dual lattice (*l dual to p) which carry a non-zero vorticity $^*\sigma_{x,\rho} = \varepsilon_{\rho\mu\nu} \sigma_{x,\mu\nu} / 2$. Those trajectories are either closed or begin/end on Nambu (anti-) monopoles.

3. Vortex profiles

The topologically unstable vortices populate the “vacuum” of the model due to thermal fluctuations. Looking at realistic equilibrium configurations [12] we would not expect to find vortices with classical (ANO type, Refs. [10]) profiles. Our lattice vortex defect operator (1) is constructed to

*Presented by the first author at Lattice'99, Pisa, Italy.

detect a line-like object (in 3D space-time) with non-zero vorticity (“soul of the physical vortex”). Within a given gauge-Higgs configuration, the vortex profile around that soul would be screened by quantum fluctuations, compared to its classical shape. However, the average over all vacuum vortices may reveal a structure resembling a classical vortex to some extent. This requires to study the correlators of the vortex operators with various field operators. Profiles obtained in this way are called “quantum vortex profiles” although *thermal* fluctuations contribute to the correlators, too.

Preliminary indications of some vortex-like structure have been given in Ref. [6]. While in the center of a classical *continuum* vortex the Higgs field modulus is zero and the energy density reaches its maximum [3,2], in thermal equilibrium *on the lattice* the (squared) modulus of the Higgs field, $\rho^2 = (\phi_x^+ \phi_x)$ (the gauge field energy density, $E^g = 1 - \frac{1}{2} \text{Tr} U_p$) were found lower (higher) on the vortex trajectories than the corresponding bulk averages².

We define the following vortex-field correlators for plaquettes P_0 and P_R located in the same plane (perpendicular to a local segment of the vortex trajectory)

$$C_\rho(R) = \langle \sigma_{P_0}^2 \rho_{P_R}^2 \rangle, \quad C_E(R) = \langle \sigma_{P_0}^2 E_{P_R}^g \rangle, \quad (2)$$

where R is the distance between the plaquettes. The Higgs modulus is $\rho_P^2 = (1/4) \sum_{x \in P} \rho_x^2$ (averaged over the corners of P).

The quantum vortex profiles for the Higgs field, $C_\rho(R)$, and gauge field energy, $C_E(R)$, are shown in Figures 1(a) and 1(b), respectively, for two values of the hopping parameter: $\beta_H = .3440$ (symmetric side) and $\beta_H = .3536$ (on top of the crossover) for a lattice 16^3 at gauge coupling³ $\beta_G = 8$. On the Higgs side the profiles are qualitatively similar. One can see from these Figures that the vortices have, on the average, a thickness of several lattice spacings while the center of the vortex is located within the plaquette P_0 [identified by the vortex current (1)].

²A similar method was used to study the physical features of Abelian monopoles in $SU(2)$ gluodynamics, Ref. [13].

³Results for larger β_G and bigger lattices will be presented elsewhere.

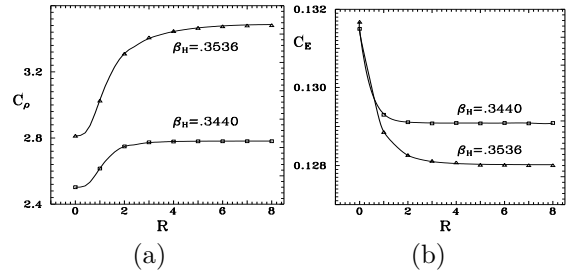


Figure 1. Examples of vortex profiles for the Higgs field (a) and gauge field energy (b). Solid lines represent fits (3).

To parametrize the vortex shape we fit the correlator data (2) by the following functions:

$$C_\rho^{\text{fit}}(R) = C_\rho + B_\rho \sum_{x \in P_0, y \in P_R} G(|\mathbf{x} - \mathbf{y}|; m_\rho),$$

$$C_E^{\text{fit}}(R) = C_E + B_E G(R; m_E) \quad (3)$$

with asymptotic values $C_{\rho,E}$ as well as amplitudes $B_{\rho,E}$ and inverse coherence lengths (effective masses) m_E and m_ρ . The *lattice* function $G(R; m)$ was proposed to fit *point-point* correlation functions in Ref. [14]. The function G is proportional to the scalar propagator with the mass $2 \sinh(m/2)$ in 3D space. Best fits are shown in Figures 1 by solid lines.

As an example, the effective masses as function of the hopping parameter (decreasing temperature) are shown in Figures 2 on the sym-

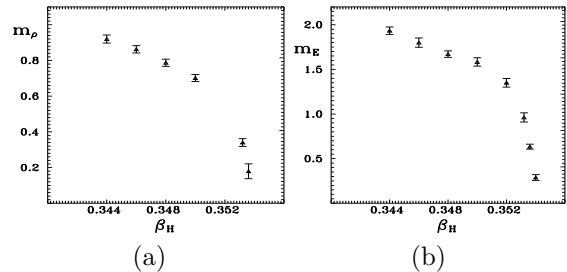


Figure 2. Fitted mass parameters of the quantum vortex Higgs (a) and energy (b) profiles.

metric side of the crossover. The masses become small near the crossover (where the fit ceases to be good). Deeper on the symmetric side, the quantum vortex profiles are squeezed compared

to the classical ones due to Debye screening leading to a smaller coherence length. Approaching the crossover from the symmetric side the density of the vortices becomes smaller reducing this effect.

4. Type of vortex vacuum

A vortex medium can be characterized in superconductor terms: if two static vortices with the same vorticity attract (repel) each other the medium corresponds to a type-I (type-II) superconductor. In order to define the type of interaction for the case of electroweak matter we have measured two-point functions of the vortex currents:

$$\begin{aligned} C_+(R) &= \langle |\sigma_{P_0}| |\sigma_{P_R}| \rangle = 2(g_{++} + g_{+-}) \\ C_-(R) &= \langle \sigma_{P_0} \sigma_{P_R} \rangle = 2(g_{++} - g_{+-}) \end{aligned} \quad (4)$$

where $g_{\pm\pm} = g_{\pm\pm}(R)$ is shorthand for contributions to the correlation functions C_{\pm} of parallel or anti-parallel vortices at positions P_0 and P_R . Obviously, $g_{++} = g_{--}$ and $g_{+-} = g_{-+}$.

The correlators $g_{++}(R) = (C_+ + C_-)/4$ ($g_{+-}(R) = (C_+ - C_-)/4$) can be interpreted as the average density of vortices (anti-vortices) relative to the bulk density (normalized to unity at $R \rightarrow \infty$) in the plane orthogonal to a vortex current at distance R .

If the vortices attract/repel each other (type-I/type-II) the long range tail of the function $g_{++}(R)$ should exponentially approach unity from above/below, while the behavior of $g_{+-}(R)$ is attractive independent of the type of superconductivity.

In Figure 3 one can see that the same-

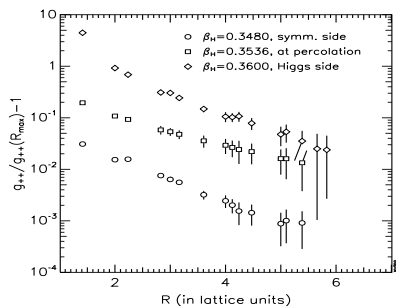


Figure 3. Normalized correlator $g_{++}(R)$.

vorticity pair distribution g_{++} ⁴ decreases exponentially with a slope that becomes minimal on the crossover. Apart from $R < 2$ the opposite-vorticity distribution g_{+-} behaves similarly. Thus we conclude that electroweak matter at the crossover belongs to the type-I vortex vacuum class. The attractive character becomes even stronger on the Higgs (lower temperature) side.

Acknowledgments

M.N. Ch. was partially supported by grants INTAS-RFBR-95-0681, RFBR-99-01230a and INTAS 96-370.

REFERENCES

1. T. Vachaspati and M. Barriola, *Phys. Rev. Lett.* **69** (1992) 1867.
2. M. Barriola, T. Vachaspati, M. Bucher, *Phys. Rev.* **D50** (1994) 2819.
3. Y. Nambu, *Nucl. Phys.* **B130** (1977) 505.
4. N.S. Manton, *Phys. Rev.* **D28** (1983) 2019.
5. M.N. Chernodub, F.V. Gubarev, E.-M. Ilgenfritz, A. Schiller, *Phys. Lett.* **B434** (1998) 83.
6. M.N. Chernodub, F.V. Gubarev, E.-M. Ilgenfritz, A. Schiller, *Phys. Lett.* **443** (1998) 244.
7. K. Kajantie et al., *Nucl. Phys.* **B458** (1996) 90; M. Gürtler et al., *ibid.* **B483** (1997) 383.
8. K. Kajantie, M. Laine, K. Rummukainen, M. Shaposhnikov, *Nucl. Phys.* **B493** (1997) 413.
9. K. Kajantie et al., *Phys. Rev. Lett.* **77** (1996) 2887; M. Gürtler, E.-M. Ilgenfritz, A. Schiller, *Phys. Rev.* **D56** (1997) 3888.
10. A.A. Abrikosov, *Sov. Phys. JETP* **32** 1442 (1957); H.B. Nielsen and P. Olesen, *Nucl. Phys.* **61** (1973) 45.
11. M.N. Chernodub, F.V. Gubarev, E.-M. Ilgenfritz, *Phys. Lett.* **B424** (1998) 106.
12. M.N. Chernodub, F.V. Gubarev, E.-M. Ilgenfritz, A. Schiller, [hep-ph/9902285](https://arxiv.org/abs/hep-ph/9902285).
13. B.L.G. Bakker, M.N. Chernodub, M.I. Polikarpov, *Phys. Rev. Lett.* **80** (1998) 30.
14. J. Engels, V.K. Mityushkin, T. Neuhaus, *Nucl. Phys.* **B440** (1995) 555.

⁴Shortest distances and data points of the order of the noise have been omitted.